ISSN 1070-3284, Russian Journal of Coordination Chemistry, 2022, Vol. 48, No. 11, pp. 733–740. © Pleiades Publishing, Ltd., 2022.
Russian Text © The Author(s), 2022, published in Koordinatsionnaya Khimiya, 2022, Vol. 48, No. 11, pp. 677–685.

# Spin Transition of the Iron(II) Clathrochelate in the Photopolymer Composition for 3D Printing from Optical Spectroscopy Data

**A. I. Cherevko[a], R. R. Aisin[a], A. S. Belov[a], S. A. Belova[a], and Yu. V. Nelyubina[a, *]**

[a] *Nesmeyanov Institute of Organoelement Compounds, Russian Academy of Sciences, Moscow, 119991 Russia*

**e-mail: unelya@ineos.ac.ru*

Received April 25, 2022; revised May 27, 2022; accepted May 30, 2022

**Abstract**—The spin state of the previously described iron(II) clathrochelate in two photopolymer compositions for 3D printing is studied for the first time by ultraviolet–visible (UV–Vis) spectroscopy. The photopolymer compositions are shown to favor the temperature-induced spin transition that becomes sharper than that in solutions or in crystalline films of this complex. A possibility of preparing objects of complicated shape and internal geometry using photopolymer 3D printing from the compositions containing compounds with spin transitions provides broad prospects for their use in devices of soft robotics, for example, as actuators.

**Keywords:** clathrochelates, composite materials, temperature-induced spin transition, UV–Vis spectroscopy, photopolymer 3D printing

**DOI:** 10.1134/S1070328422110033

## INTRODUCTION

Some complexes of transition metals with the $d^4$–$d^7$ electronic configuration can exist in two spin states and can be switched between them under the application of an appropriate external stimulus (e.g., temperature or pressure) [1]. A similar spin transition is accompanied by significant changes in the magnetic, optical, mechanical, and other properties of these compounds, which allows one to manufacture from them various devices and materials [2, 3], including sensors [4], and elements in devices of molecular spintronics [5] and soft robotics [6] have been produced since recently. In the last case, the corresponding compounds (as a rule, metal-organic frameworks [7, 8]) that undergo the spin transition in bulky crystalline samples are introduced in a polymer composite thus providing a possibility of forming materials and even units of required shapes and sizes [6]. These composites are widely used, for instance, for the preparation of functional layers of storage devices [7] or generators and actuators for soft robotics devices [9], including using photopolymer 3D printing [10]. As other methods of 3D printing [11], the latter implies the reproduction of a digital model by the layer-to-layer extrusion of the polymer material [12], namely, the photosensitive resin [13]. Owing to the use of the resin for the layer-to-layer polymerization of projectors with a high resolution, photopolymer 3D printing makes it possible to produce objects with a high spatial resolution. In particular, the light-cured resin is actively used for the production of functional objects for catalysis [14], medicine [15], gas adsorption and storage [16], and other practically important applications [17].

One of the classes of compounds undergoing the temperature-induced spin transition [18, 19] is formed by macrobicyclic tris(dioximate) cell complexes (clathrochelates [20]) of cobalt(II). In addition to high thermal and chemical stabilities, these compounds are characterized by a simple synthesis and broad possibilities of chemical modification (at two apical and four ribbed positions of the cell ligand) that make it possible to control their magnetic properties [21] using molecular design. In particular, this allowed us to synthesize the first iron(II) clathrochelate (**I**) (Scheme 1) capable of changing its spin state triggered by an external stimulus [22]. However, the corresponding spin transition occurred in solutions of complex **I** rather than in the bulky crystalline samples or crystalline films [22], which substantially shortens a possible range of practical applications of this unique class of coordination compounds.

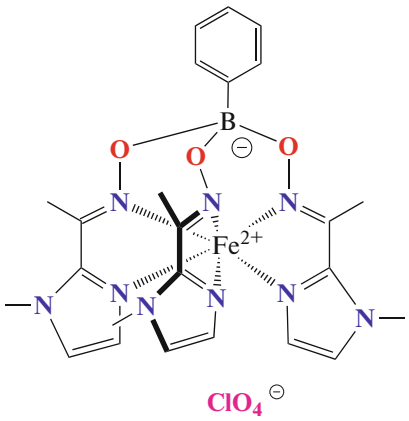


**(I)**

**Scheme 1.**

This problem can be solved by the use of composite materials in which clathrochelate particles are distributed in the polymer matrix acting as a solvent [6]. This approach can provide the temperature-induced spin transition in the solid state and also manufacturing "switchable" functional materials [23–25] or elements [9, 10, 26] using photopolymer 3D printing [10].

In this work, we prepared the photopolymer compositions containing complex **I** based on the commercial resin for 3D printing HARZ LABS Model Resin (Russia) and previously developed by us original resin [27] and studied the spin state in the films using UV-VIS spectroscopy at different temperatures.

## EXPERIMENTAL

All procedures were carried out in air using commercially available reagents, organic solvents, and sorbents. 2-Acetyl-1-methylimidazole oxime was synthesized using a previously described procedure [28] from 2-acetyl-1-methylimidazole [29]. Analyses to the contents of carbon, nitrogen, and hydrogen were carried out on a Carlo Erba microanalyzer (model 1106). The iron content was determined by X-ray fluorescence analysis. $^1$H NMR spectra were recorded in $CD_2Cl_2$ on a Bruker Avance 300 FT spectrometer ($^1$H frequency was 300.13 MHz). Chemical shifts were measured relative to the residual signal of the solvent ($^1$H 5.32 ppm).

**Synthesis of complex I.** 2-Acetyl-1-methylimidazole oxime (1.85 g, 13.3 mmol) and phenylboronic acid (0.56 g, 4.6 mmol) were dissolved in ethanol (40 mL) with stirring under an argon atmosphere. Then $NaClO_4 \cdot H_2O$ (2.67 g, 19 mmol), $NaHCO_3$ (0.96 g, 11.4 mmol), and $FeCl_2 \cdot 4H_2O$ (0.76 g, 3.8 mmol) were added consecutively. The reaction mixture was refluxed with stirring for 1 h and cooled to room temperature. The formed red-orange precipitate was washed with ethanol (20 mL, 4 portions) and diethyl ether (10 mL) and extracted with acetonitrile (20 mL, 4 portions). The extract was evaporated to dryness and dried in vacuo The yield was 2.35 g (94%).

| For $C_{24}H_{29}N_9O_7BClFe$ | | | | |
|---|---|---|---|---|
| Anal. calcd., % | C, 43.80 | H, 4.41 | N, 19.17 | Fe, 8.52 |
| Found, % | C, 43.30 | H, 4.44 | N, 19.04 | Fe, 8.73 |

$^1$H NMR (300.13 MHz; $CD_2Cl_2$; 190 K; δ, ppm): 7.67 (br.s, 2H, *ortho*-Ph), 7.31 (br.s, 3H, *para*-Ph, *meta*-Ph), 7.15 (br.s, 3H, 5-Imd), 6.37 (br.s, 3H, 4-Imd), 3.96 (br.s, 9H, $CH_3$), 2.66 (br.s, 9H, $CH_3$-Imd).

To prepare crystalline films, a dry crystalline powder of complex **I** (20 mg) was dissolved in acetonitrile or dichloromethane (300 μL), and the solution was filtered through the Celite layer. The films were deposited onto quartz supports by casting of the obtained solution (10 μL) at room temperature with a rate of 1 cm/min and then dried at room temperature in vacuo ($10^{-2}$ Torr) for 30 min.

Complex **I** (40 mg) was dissolved in acetonitrile (1 mL) to prepare the photopolymer composition based on the commercial resin for 3D printing. The HARZ LABS Model Resin commercial resin for 3D printing (4 g) was added to the obtained solution, and the mixture was stirred with an ultrasonic homogenizer for 5 min.

The original resin for 3D printing was prepared using a previously described procedure [27] by mixing 2-phenoxyethyl acrylate (2.38 g), trimethylpropanetriacrylate (2.38 g), hydroxycyclohexyl phenyl ketone (0.25 g), and phenylbis(2,4,6-trimethylbenzoyl)phosphine oxide (0.13 g). The resulting mixture was stirred with an ultrasonic homogenizer for 5 min.

Complex **I** (40 mg) was dissolved in acetonitrile (1 mL) to prepare the photopolymer composition based on the original resin for 3D printing. The original resin for 3D printing (4 g) was added to the resulting solution, and the mixture was stirred with an ultrasonic homogenizer for 5 min.

To prepare polymer films, the photopolymer composition containing the HARZ LABS Model Resin commercial resin or original resin with 1 wt % complex **I** was uniformly deposited as 3–4 layers on a quartz support with a brush. Each layer was solidified using a UV lamp at the wavelength 370 nm for 1–2 min. The obtained film was washed with isopropyl alcohol.

The UV–Vis spectra of the prepared films of complex **I** were recorded in a range of 350–600 nm on a Carl Zeiss Jena Specord M400 spectrophotometer in a vacuum cryostat ($10^{-2}$ Torr), which was filled with argon, in a temperature range of 298–423 K.

Scanning electron microscopy (SEM) images for the sample placed on a 25-mm aluminum stage and fixed with a conducting carbon ribbon were detected

on a TM4000 Plus instrument in the secondary electron mode at an accelerating voltage of 5–15 kV.

A WANHAO DUPLICATOR 7 photopolymer 3D printer was used for 3D printing from the photopolymer composition containing the original resin with 1 wt % complex **I** using the DLP (Digital Light Processing) technology at the following parameters: the light-striking time of the layer was 150 s and the layer thickness was 0.01 mm.

## RESULTS AND DISCUSSION

Complex **I** was synthesized using a previously described procedure [22] by the direct template reaction of 2-acetyl-1-methylimidazole oxime, phenylboronic acid, and iron(II) chloride in boiling ethanol (Scheme 2). The complex was isolated in the individual form in a high yield and characterized by elemental analysis and NMR spectroscopy.

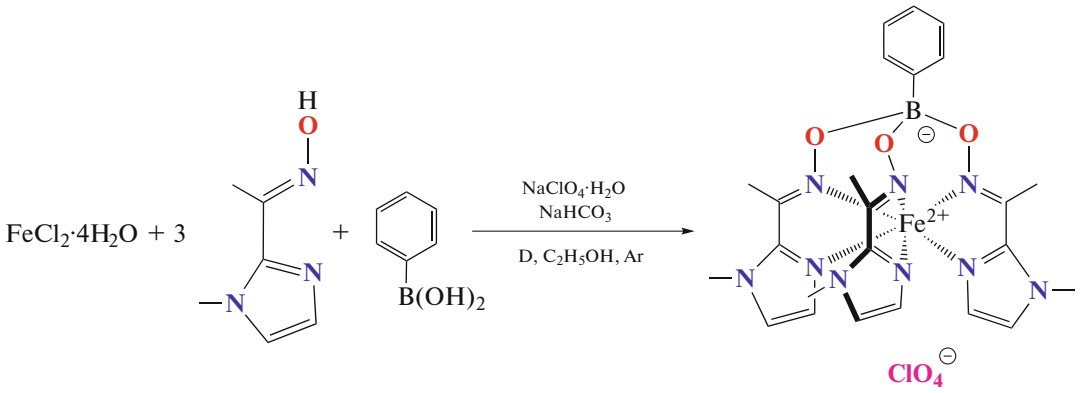


**(I)**

**Scheme 2.**

According to the previously obtained NMR spectroscopy and UV–Vis spectroscopy data [22], complex **I** retained its integrity on heating to 343 K in solutions of acetonitrile and dichloromethane and underwent a very smooth spin transition started at the temperature slightly above room temperature. No spin transition is observed on heating up to 353 K of the bulky crystalline samples or films formed from the indicated solutions. It should be mentioned that the choice of the upper temperature was determined by a potential explosion hazard of crystalline perchlorates.

The problem can be solved by the preparation of composite materials in which a minor amount of complex **I** (e.g., 1 wt %) is distributed over the polymer matrix. The commercial resin for photopolymer 3D printing (HARZ LABS Model Resin, Russia) and the original resin prepared by us [27] were used as polymer matrices for manufacturing such composites. Although complex **I** was highly soluble in both the commercial and original resins, the presence of only 1 wt % of the complex strongly affected the color of the photopolymer compositions, which exerts a negative effect on the quality and other important parameters of photopolymer 3D printing [30]. According to the SEM data, the polymerization of both photopolymer compositions containing 1 wt % complex **I** affords homogeneous polymer films (with minor defects as bubbles and traces from the brush used for deposition) in which particles of the complex are uniformly distributed over the polymer matrix (Fig. 1).

The polymer films formed by the layer-to-layer deposition (lamination) of these compositions on quartz supports were studied by UV–Vis spectroscopy in the temperature range from 298 to 423 K (Fig. 2). At room temperature, clathrochelate **I** exists predominantly in the low-spin (LS) state in these films, which corresponds to the metal–ligand charge-transfer band with a maximum about 476 nm in the visible range. The band is slightly (by 6 nm) shifted to the red range relative to the spectra of solutions [22] in which its half-width varies from 3600 to 3700 $cm^{-1}$, whereas in

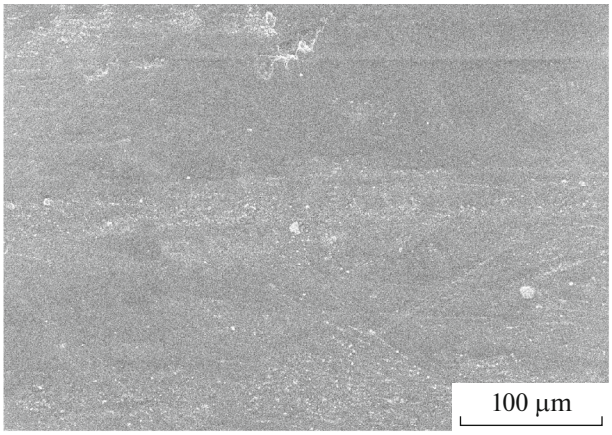


**Fig. 1.** SEM image for the film of the photopolymer composite containing the original resin with 1 wt % complex **I**.

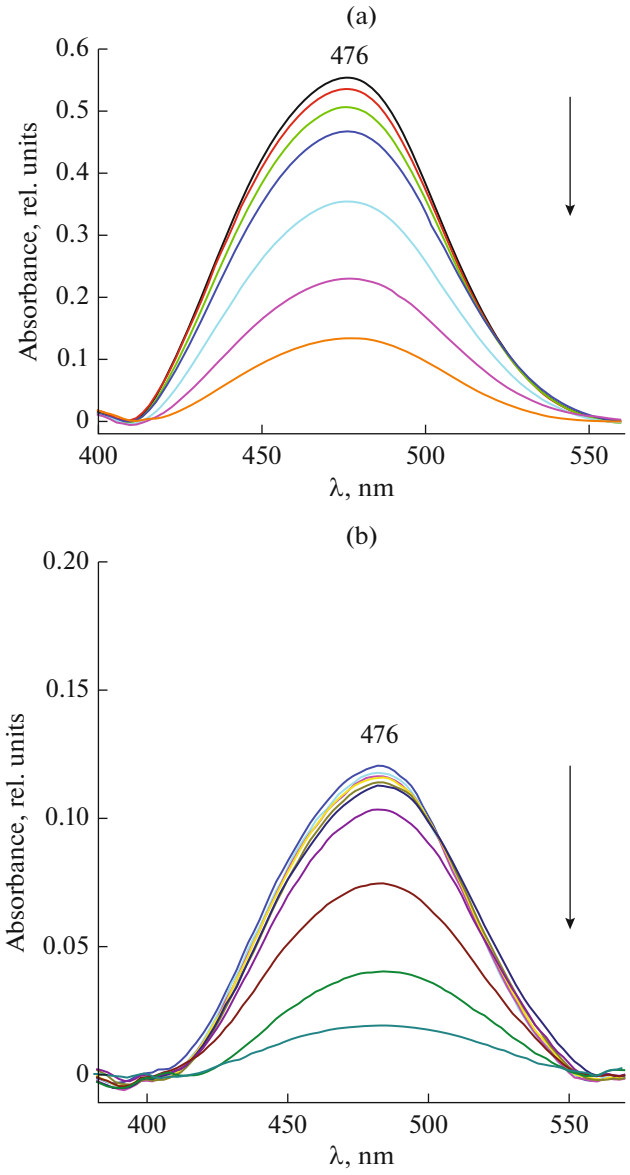


**Fig. 2.** Temperature dependences of the UV–Vis spectrum for the films of the photopolymer compositions containing the (a) HARZ LABS Model Resin commercial resin and (b) original resin with 1 wt % complex **I** on heating from room temperature to 423 K with an increment of 25 K.

the polymer films this band lies at 3050 and 3300 $cm^{-1}$ for the HARZ LABS Model Resin commercial resin and original resin, respectively.

The heating of the films led to a fairly sharp decrease in the metal–ligand charge-transfer band intensity, indicating the population of the high-spin (HS) state of the iron(II) ion already at temperatures close to room temperature. In this case, the observed temperature-induced spin transition remained incomplete even at 423 K.

The prepared films noticeably differ from each other and from solutions of the complex by the temperature and completeness of the spin transition. Although the absence of UV–Vis spectra for individual spin states does not allow one to directly determine the transition temperature, the transition onset can approximately be determined from the inflection of the curve of changing the metal–ligand charge-transfer band intensity (Fig. 3). The corresponding inflection is observed at temperatures about 315, 360, and 380 K for a solution of the complex in acetonitrile and polymer films of the HARZ LABS Model Resin commercial resin and original resin, respectively. The lowest value expectedly corresponds to the solution in which the rearrangement of the molecular structure of the complex for the transition from the LS to HS state is least impeded (the changes in the UV–Vis spectra on heating to 315 K are due to a natural decrease in the intensity and absorption band broadening) and is completely consistent with the NMR spectroscopy data [22] for a similar solution indicating a very smooth spin transition above this temperature. On the contrary, the transition in the films is observed at higher temperatures and characterized by pronounced cooperativity (especially in the case of the HARZ LABS Model Resin commercial resin), which is seen from a decrease in the metal–ligand charge-transfer band intensity on heating (Fig. 3). A similar cooperativity characteristic of the crystalline materials is evidently caused by the influence of the solid photopolymer compositions in which particles of complex **I** are uniformly distributed.

A decrease in the temperature of the polymer films to room temperature resulted in their cracking because of the difference in the thermal expansion coefficients of the polymer and quartz support. The polymer based on the HARZ LABS Model Resin commercial resin underwent especially strong cracking and, hence, the UV–Vis spectra were recorded on cooling only for the film obtained using the original photopolymer resin (Fig. 4a). They demonstrate only an insignificant increase in the metal–ligand charge-transfer band intensity related to a natural increase in the intensity and a decrease in the absorption band width. Moreover, a series of the subsequent heatings and coolings (Fig. 4b) resulted in the situation where the intensity of this band in the UV–Vis spectra decreased in the whole temperature range. This implies that complex **I** does not return to the initial LS state after heating the polymer composition to 423 K and remains high-spin even at room temperature, which has previously been observed only in one of its crystalline solvates with acetonitrile according to the X-ray diffraction data [22].

Since the primary heating of the polymer films triggers the spin transition at the temperatures above the maximum value (353 K) used for recording the UV–Vis spectra of the crystalline films of complex **I**, the latter were repeatedly examined in the temperature range 298–423 K. The crystalline films were prepared by casting of solutions of the complex in acetonitrile

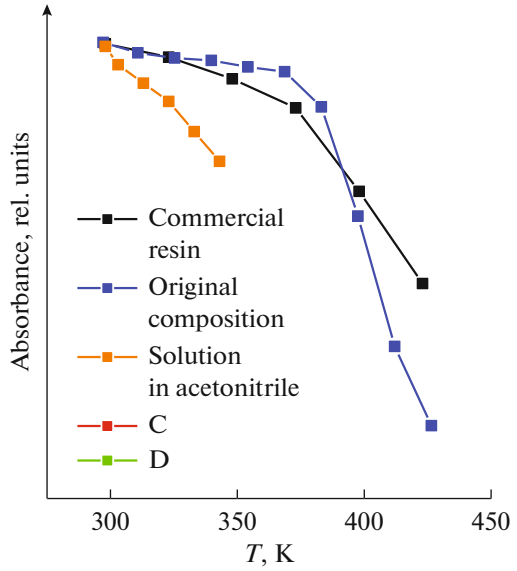


**Fig. 3.** Temperature dependence of the metal–ligand charge-transfer band intensity in the UV–Vis spectra of the polymer films of complex **I** on heating. The UV–Vis spectra for the solution were recorded in a range of 303–343 K with an increment of 10 K [22].

and dichloromethane on the surface of quartz supports, which resulted in the formation of uniform films according to the SEM data (Fig. 5). The films retained the structure on the surface under the vacuum cryostat conditions ($10^{-2}$ Torr), which is indicated by a similarity of their UV–Vis spectra at room temperature (Fig. 6) and the corresponding spectra for solutions [22] and films of the photopolymer compositions (Fig. 2).

However, a noticeable decrease in the intensity of the band with a maximum about 474 $cm^{-1}$ is observed only on heating the crystalline films above 353 K (Fig. 5), which explains the earlier conclusion about the absence of a temperature-induced transition below 353 K. According to the inflection on the curve of changing intensity, the both films demonstrate the temperature of the transition onset (360 K) approximately equal to that for the polymer film from the HARZ LABS Model Resin commercial photopolymer resin. However, they exhibit no analogous cooperativity in a temperature range of 298–423 K (Fig. 7). The HS state in them is populated on heating even more slowly than in solutions of complex **I**.

Moreover, the behavior of complex **I** in the crystalline films differs substantially from that in the polymer films followed by cooling to room temperature (Fig. 8). If complex **I** remains high-spin, it almost completely returns to the initial state. The hysteresis of this temperature-induced spin transition is observed about 75 K, which is due, most likely, to the accompanying strong rearrangement that can both induce a sharp spin transition with the hysteresis [31] and stabi-

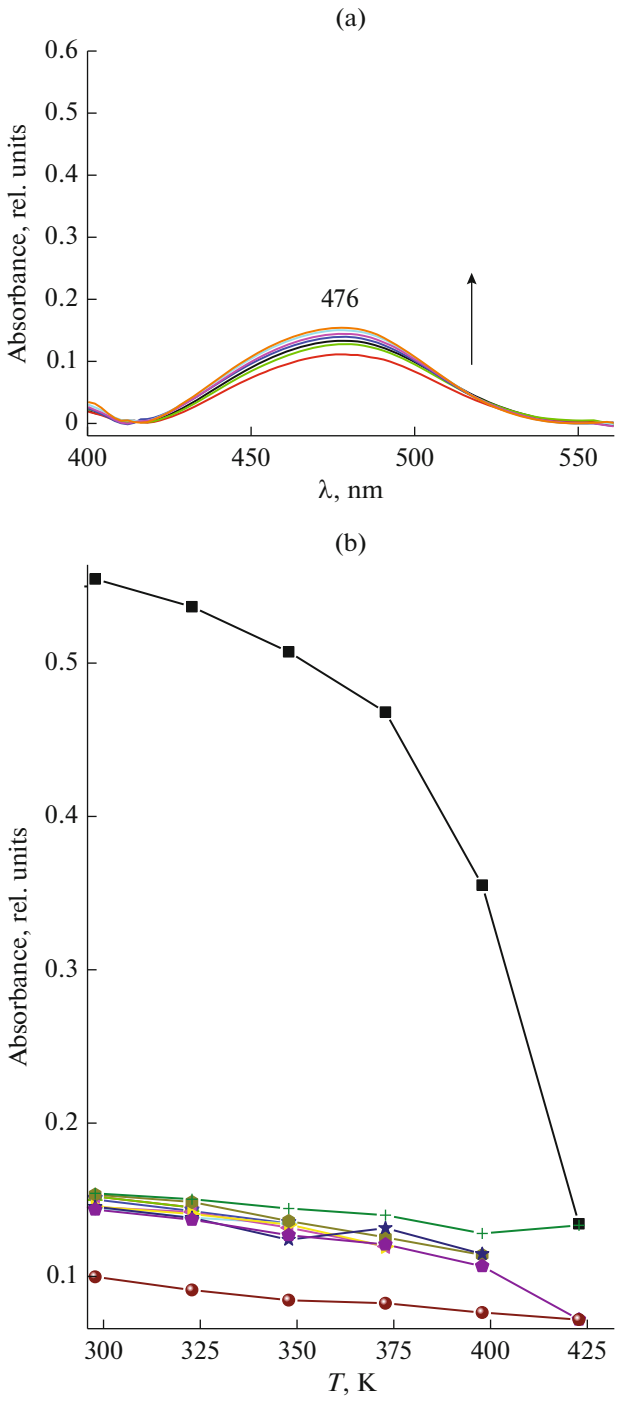


**Fig. 4.** (a) Temperature dependences of the UV–Vis spectrum and (b) metal–ligand charge-transfer band intensity for the film of the photopolymer composition containing the HARZ LABS Model Resin commercial resin with 1 wt % complex **I** for the consecutive series heating–cooling to 423, 323, 348, 373, 398, and 423 K.

lize only one of the spin states [32, 33]. In fact, during the spin transition complex **I** should appreciably change its coordination geometry that, according to the X-ray diffraction data for different solvatomorphs

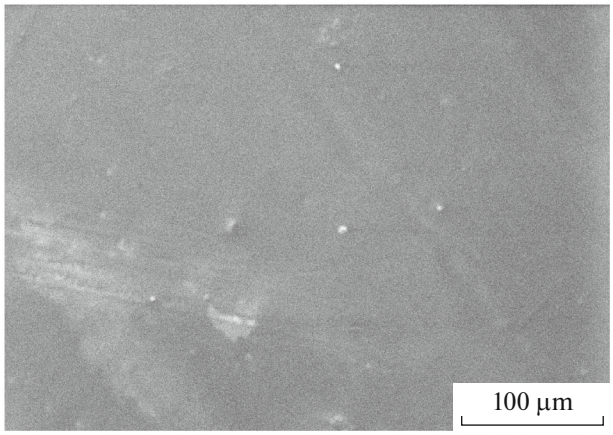


**Fig. 5.** SEM image of the crystalline film prepared by casting of a solution of the complex in acetonitrile.

of complex **I** [22], is close to a trigonal antiprism in the LS state and is an almost ideal trigonal prism in the HS state.

The differences observed in the spin transition parameters of the crystalline and polymer films of complex **I** indicate different effects of its crystal packing and photopolymer matrices used, the choice of which makes it possible to control the spin transition parameters, for instance, temperature and hysteresis [6]. They also can make it sharper as the HARZ LABS Model Resin commercial resin for 3D printing or self-made original resin [27], which is desirable for the majority of practical applications [2, 31, 34–36] of the compounds with spin transitions as sensors and components of molecular spintronics and soft robotics devices.

We tested the corresponding photopolymer compositions containing 1 wt % complex **I** by the digital light processing (DLP) method under the 3D printing conditions for various objects (Fig. 9). As mentioned above, this complex acts as both the functional additive and strong dye, which significantly restricts its limiting concentration in the composition for photopolymer 3D printing due to the essence of the photopolymerization process. To be capable of polymerizing, the photopolymer resin should accept a certain energy dose (UV radiation), and the dye acts, in this case, as the absorber of this energy [30]. A strong absorption of UV radiation directly affects both the quality of photopolymer 3D printing and the possibility of preparing objects by this method. Indeed, the presence of even 1 wt % complex **I** in the photopolymer compositions based on the commercial or original resin stains them so strongly that the production of objects thicker than 1 mm becomes possible only with a considerable loss of 3D printing quality, for example, by changing the geometry or a decrease in specified linear sizes of the units. A good result of photopolymer 3D printing was reached for the objects with the thickness to 1 mm by the elongation of the exposure time to 120 s per layer, whereas the normal exposure time of the pure photopolymer is 10 s.

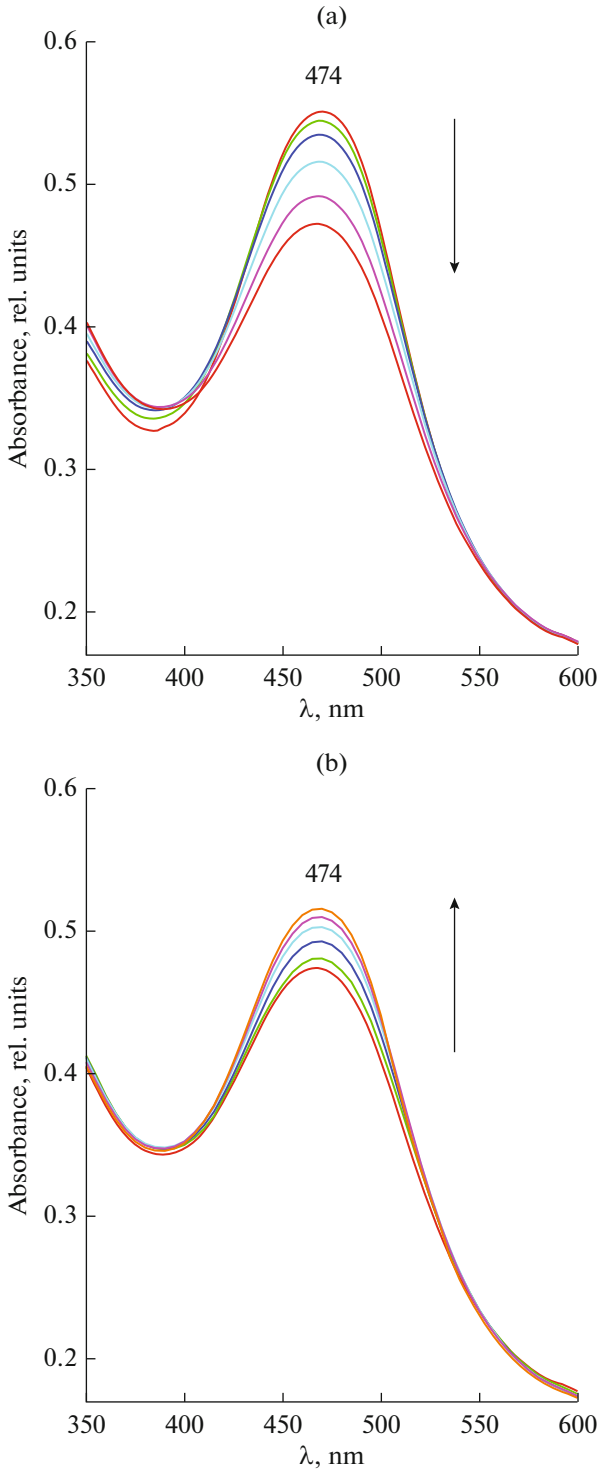


**Fig. 6.** Temperature dependences of the UV–Vis spectrum for the film prepared by casting of a solution of the complex in dichloromethane on (a) heating and (b) consecutive cooling in the temperature range from 298 to 423 K with an increment of 25 K.

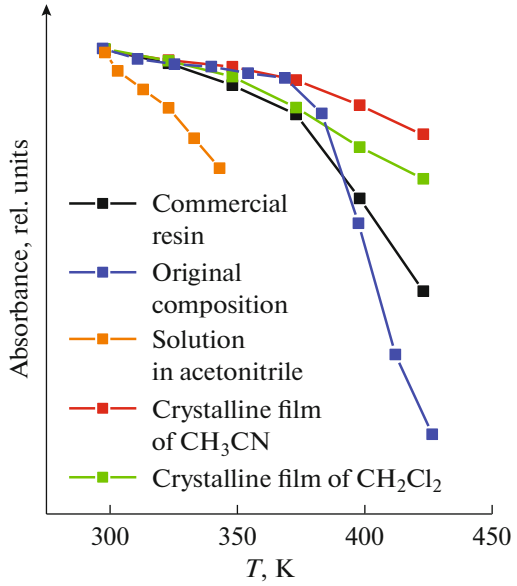


**Fig. 7.** Temperature dependences of the metal–ligand charge-transfer band intensity in the UV–Vis spectra of the crystalline and polymer films of complex **I** and its solution in acetonitrile on heating.

Thus, the spin state of the previously described iron(II) clathrochelate was studied in the wide temperature range. It turned out that the temperature-induced spin transition for the chosen clathrochelate **I**, which retained its integrity on depositing on the surface and on heating to 423 K, was observed in both the solutions and crystalline films. In these films, however, the spin transition starts at appreciably higher temperatures and is characterized by negative cooperativity [19]; i.e., it occurs even more smoothly than in solutions. On the contrary, in the polymer films of the photopolymer compositions containing only 1 wt % complex **I**, the spin transition becomes much sharper as required by the majority of practical applications [2, 31, 34–36] of complex compounds with spin transitions. A possibility to control the spin transition parameters by the introduction of these compounds into the photopolymer compositions and selection of the compositions for photopolymer 3D printing, which allows high-precision manufacturing three-dimensional objects of complicated shape and internal geometry, provides broad prospects for their use as components in soft robotics devices, for example, actuators [9, 26].

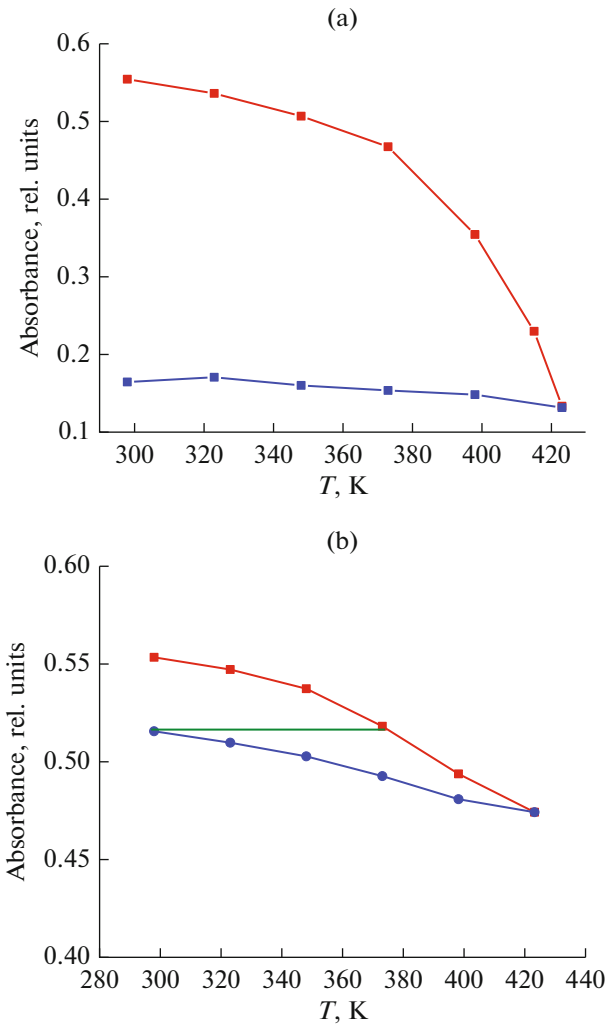


**Fig. 8.** Temperature dependences of the metal–ligand charge-transfer band intensity in the UV–Vis spectra of the film prepared (a) by casting of a solution of the complex in dichloromethane and (b) from the photopolymer composition containing the HARZ LABS Model Resin commercial resin with 1 wt % complex **I** on heating (red curve) and subsequent cooling (blue curve) in the temperature range from 298 to 423 K with an increment of 25 K. Green line corresponds to the hysteresis of the transition.

## ACKNOWLEDGMENTS

Elemental analysis was carried out using the scientific equipment of the Center of Investigation of Structure of Molecules at the Nesmeyanov Institute of Organoelement Compounds (Russian Academy of Sciences).

## FUNDING

This work was supported by the Russian Science Foundation, project no. 19-73-10194.

## CONFLICT OF INTEREST

The authors declare that they have no conflicts of interest.

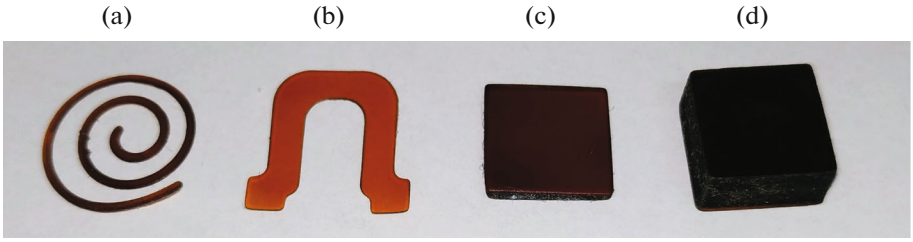


**Fig. 9.** Objects prepared using 3D printing from the photopolymer composition containing the original resin with 1 wt % complex **I**: (a) coil 0.5 mm thick, (b) cantilever 0.3 mm thick, and parallelepipeds (c) 1.4 mm and (d) 5 mm thick. Exposure time: (a, b) 120 s per layer and (c, d) 150 s per layer.

## REFERENCES


1. *Spin-Crossover Materials: Properties and Applications*, Halcrow, M.A., Ed., Chichester: Wiley, 2013.
2. Molnár, G., Rat, S., Salmon, L., et al., *Adv. Mater.*, 2017, vol. 30, no. 5, p. 1703862.
3. Senthil Kumar, K. and Ruben, M., *Coord. Chem. Rev.*, 2017, vol. 346, p. 176.
4. Linares, J., Codjovi, E., and Garcia, Y., *Sensors*, 2012, vol. 12, p. 4479.
5. Coronado, E., *Nature Rev. Mat.*, 2020, vol. 5, no. 2, p. 8704.
6. Enriquez-Cabrera, A., Rapakousiou, A., Piedrahita Bello, M., et al., *Coord. Chem. Rev.*, 2020, vol. 419, p. 213396.
7. Koo, Y.-S. and Galán-Mascarós, J.R., *Adv. Mat.*, 2014, vol. 26, no. 39, p. 6785.
8. Nguyen, M.T., Jones, R.A., and Holliday, B.J., *Polymer*, 2021, vol. 222, p. 123658.
9. Piedrahita-Bello, M., Zan, Y., Enriquez-Cabrera, A., et al., *Chem. Phys. Lett.*, 2022, vol. 793, p. 139438.
10. Piedrahita-Bello, M., Angulo-Cervera, J.E., Courson, R., et al., *J. Mat. Chem.*, 2020, vol. 8, no. 18, p. 6001.
11. Kantaros, A., Diegel, O., Piromalis, D., et al., *Mat. Today: Proceed*, 2022, vol. 49, p. 2712.
12. Femmer, T., Flack, I., Wessling, M., et al., *Chem. Ing. Tec.*, 2016, vol. 88, p. 535.
13. Scott, P.J., Meenakshisundaram, V., Hegde, M., et al., *ACS Appl. Mat. Inter.*, 2020, vol. 12, p. 10918.
14. Zhou, X. and Liu, C., *Adv. Funct. Mat.*, 2017, vol. 27, p. 1701134.
15. Awad, A., Trenfield, S.J., Gaisford, S., et al., *Int. J. Pharm.*, 2018, vol. 548, p. 586.
16. Liu, X.M., Lim, G.J.H., Wang, Y., et al., *Chem. Eng. J.*, 2021, vol. 403, p. 126333.
17. Belka, M. and Baczek, T., *TrAC Trends Anal. Chem.*, 2021, vol. 142, p. 116322.
18. Voloshin, Y.Z., Varzatskii, O.A., Novikov, V.V., et al., *Eur. J. Inorg. Chem.*, 2010, vol. 2010, p. 5401.
19. Novikov, V.V., Ananyev, I.V., Pavlov, A.A., et al., *J. Phys. Chem. Lett.*, 2014, vol. 5, p. 496.
20. Voloshin, Y., Belaya, I., and Krämer, R., *Cage Metal Complexes: Clathrochelates Revisited*, Springer Cham, 2017.
21. Pavlov, A.A., Nelyubina, Y.V., Kats, S.V., et al., *J. Phys. Chem. Lett.*, 2016, vol. 7, p. 4111.
22. Denisov, G.L., Novikov, V.V., Belova, S.A., et al., *Cryst. Growth Des.*, 2021, vol. 21, p. 4594.
23. Lee, S.W., Lee, J.W., Jeong, S.H., et al., *Synth. Metal*, 2004, vol. 142, p. 243.
24. Novio, F., Evangelio, E., Vazquez-Mera, N., et al., *Sci. Rep.*, 2013, vol. 3, p. 1708.
25. Chen, Y.-C., Meng, Y., Ni, Z.-P., et al., *J. Mat. Chem., C*, 2015, vol. 3, p. 945.
26. Piedrahita-Bello, M., Angulo-Cervera, J.E., Enriquez-Cabrera, A., et al., *Mat. Horizons*, 2021, vol. 8, p. 3055.
27. Cherevko, A.I., Nikovskiy, I.A., Nelyubina, Y.V., et al., *Polymers*, 2021, vol. 13, p. 3881.
28. Pufky-Heinrich, D., Ciesielski, M., Gharnati, L., et al., *Heterocycles*, 2010, vol. 81, p. 1811.
29. Davies, D.H., Hall, J., and Smith, E.H., *J. Chem. Soc., Perkin Trans.*, 1991, p. 2691.
30. Zhakeyev, A., Zhang, L., and Xuan, J., *3D and 4D Printing of Polymer Nanocomposite Materials*, Elsevier, 2020, p. 387.
31. Halcrow, M.A., *Chem. Lett.*, 2014, vol. 43, p. 1178.
32. Bartual-Murgui, C., Vela, S., Roubeau, O., et al., *Dalton Trans.*, 2016, vol. 45, p. 14058.
33. Nelyubina, Y.V., Polezhaev, A.V., Pavlov, A.A., et al., *Magnetochemistry*, 2018, vol. 4, p. 46.
34. *Modern Magnetic and Spintronic Materials*, Kaidatzis, A., Sidorenko, S., Vladymyrskyi, I., and Niarchos, D., Eds., Dordrecht: Springer, 2020.
35. Bartual-Murgui, C., Akou, A., Thibault, C., et al., *J. Mat. Chem., C*, 2015, vol. 3, p. 1277.
36. Bousseksou, A. and Molnár, G., *Compt. Rend. Chim.*, 2003, vol. 6, p. 1175.


*Translated by E. Yablonskaya*